

## REDUCTION OF NOISE IN THE TOTAL SOLAR IRRADIANCE

W. Finsterle, C. Fröhlich

Physikalisch-Meteorologisches Observatorium Davos, World Radiation Center  
CH-7260 Davos Dorf, Switzerland

### ABSTRACT

A multivariate spectral regression analysis technique is used to model the noise in the total solar irradiance (TSI) spectrum from PMO6-VA with the three spectral channels of the sunphotometers onboard VIRGO. We find high partial and total coherence squared of up to 0.9 between the TSI spectrum and the three spectral channels. After subtracting the coherent part from the TSI spectrum several statistically significant peaks appear below 500  $\mu\text{Hz}$  which were hidden in the original spectrum. Most of them turned out to be instrumental and/or operational, e.g. harmonics of spacecraft inherent periods. One of the remaining peaks is close to p mode  $l = 1$ ,  $n = 1$ . The others are at frequencies not predicted by standard solar models. The rather unexpected noise behavior providing such significant peaks will be discussed.

### 1. MULTIVARIATE SPECTRAL REGRESSION ANALYSIS

The multivariate spectral regression analysis (Koopmans, 1974) is trying to explain the dependent components of a multivariate vector process by its filtered independent components:

$$\mathbf{Y}(t) = \mathbf{L}(\mathbf{X}(t)) + \boldsymbol{\eta}(t) \quad (1)$$

where  $\mathbf{Y}(t) = \begin{pmatrix} Y_1(t) \\ \vdots \\ Y_p(t) \end{pmatrix}$  is a  $(q \times 1)$ -dimensional vector process of the dependent components and  $\mathbf{X}(t) = \begin{pmatrix} X_1(t) \\ \vdots \\ X_p(t) \end{pmatrix}$  is a  $(p \times 1)$ -vector process of the independent components.  $\mathbf{L}$  is a multivariate linear filter with unknown  $(q \times p)$ -dimensional transfer function  $\mathbf{B}(\lambda)$  and  $\boldsymbol{\eta}(t)$  is an unobservable  $(q \times 1)$ -dimensional vector process uncorrelated with  $\mathbf{X}(t)$ , normally called noise.

The extent of deviation of  $\mathbf{Y}(t)$  from a linear function of  $\mathbf{X}(t)$  is measured by the unknown spectral density vector  $\mathbf{f}^\eta(\lambda)$ . This vector and the transfer function  $\mathbf{B}(\lambda)$ , which indicates how the linear dependence is parcelled out to the various input and output series, are the principal parameters of interest. They are

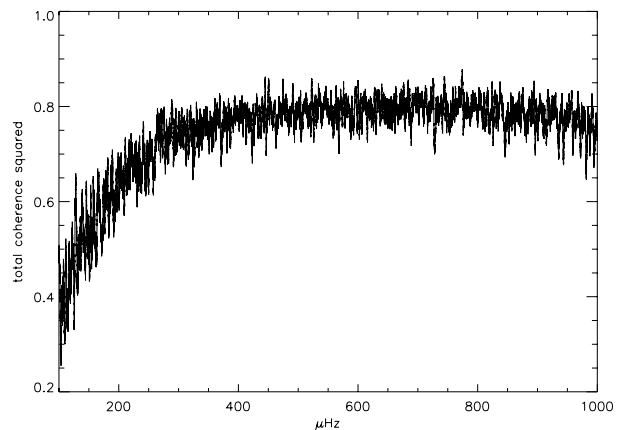


Figure 1. Total coherence squared (eq. 8) of total to spectral channels.

determined by minimizing the expectation value

$$E(\mathbf{Y}(t) - \mathbf{L}\mathbf{X}(t))^2. \quad (2)$$

The transfer function of  $\mathbf{L}$  and the spectral density function of  $\boldsymbol{\eta}(t)$  can be calculated according to

$$\mathbf{B}(\lambda) = \mathbf{f}^{Y,X}(\lambda)\mathbf{f}^{X,X}(\lambda)^{-1} \quad (3)$$

and

$$\mathbf{f}^\eta(\lambda) = \mathbf{f}^{Y,Y}(\lambda) - \mathbf{f}^{Y,X}(\lambda)\mathbf{f}^{X,X}(\lambda)\mathbf{f}^{X,Y}(\lambda)^{-1} \quad (4)$$

where  $\mathbf{f}^{X,X}(\lambda)$  and  $\mathbf{f}^{X,Y}(\lambda)$  are the power and cross spectra, respectively as  $(q \times q)$ ,  $(p \times p)$ ,  $(q \times p)$  or  $(p \times q)$  matrices

$$\mathbf{f}^{X,Y}(\lambda)d\lambda = E(\mathbf{Z}^X(d\lambda)\mathbf{Z}^Y(d\lambda)^*) \quad (5)$$

with  $\mathbf{Z}^{X,Y}(d\lambda)$  being the complex fourier amplitude of the vector process  $\mathbf{X}(t)$  or  $\mathbf{Y}(t)$ , respectively. The partial coherences  $\rho(\lambda)$  can be calculated from the  $(p \times q)$  complex coherence

$$\gamma(\lambda) = \mathbf{f}^{X,X}(\lambda)^{-\frac{1}{2}}\mathbf{f}^{X,Y}(\lambda)\mathbf{f}^{Y,Y}(\lambda)^{-\frac{1}{2}} \quad (6)$$

where  $\mathbf{A}^{-\frac{1}{2}}$  denotes the square root of the inverse of the matrix  $\mathbf{A}$ , by

$$\begin{aligned} \rho^2(\lambda) &= \gamma(\lambda)^*\gamma(\lambda) \\ &= \mathbf{f}^{Y,Y}(\lambda)^{-\frac{1}{2}}\mathbf{f}^{Y,X}(\lambda)^{-1}\mathbf{f}^{X,Y}(\lambda)\mathbf{f}^{Y,Y}(\lambda)^{-\frac{1}{2}} \end{aligned} \quad (7)$$

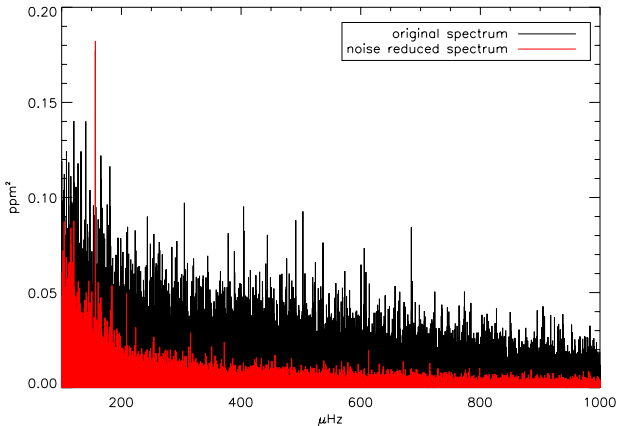


Figure 2. We used eq. 10 to reduce noise in the total solar irradiance spectrum. Unfortunately the spikes in the residual power are not due to g modes but are all instrumental. The spikes at  $156.378 \mu\text{Hz}$ ,  $208.504 \mu\text{Hz}$  and  $312.756 \mu\text{Hz}$  are the third, fourth and sixth harmonics of  $52.126 \mu\text{Hz}$  respectively, which is the beating of a spacecraft inherent and an instrumental frequency of PMO6-VA. The fourth and sixth harmonics are hidden in the noise of the original spectrum and show up only after solar noise reduction.

When the  $\mathbf{Y}(t)$  series is only 1-dimensional, i.e.  $q = 1$ , Eq. 7 yields the scalar coherence of  $Y(t)$  with  $\mathbf{X}(t)$

$$\rho^2(\lambda) = \frac{\mathbf{f}^{Y,X}(\lambda)\mathbf{f}^{X,X}(\lambda)^{-1}\mathbf{f}^{X,Y}(\lambda)}{f^{Y,Y}(\lambda)} \quad (8)$$

or the  $p$ -dimensional partial coherence vector of  $\mathbf{X}(t)$  with  $Y(t)$

$$\rho_X^2(\lambda) = \frac{\mathbf{f}^{X,X}(\lambda)^{-\frac{1}{2}}\mathbf{f}^{Y,X}(\lambda)^{-1}\mathbf{f}^{X,Y}(\lambda)}{f^{Y,Y}(\lambda)} \quad (9)$$

For the case of  $q = 1$  an IDL routine has been written which calculates the transfer function with Eq. 3 and the total and partial coherences eqs. 8, 9.

## 2. SOLAR NOISE REDUCTION

We applied the technique described above to the time series of total solar irradiance (TSI) measured by PMO6-VA and the three spectral channels of the sun-photometer (SPM) onboard VIRGO (Fröhlich et al. 1997). We set  $Y(t)$  to the TSI time series and  $\mathbf{X}(t)$  to the three spectral time series and calculate the corresponding Fourier transforms  $f^t(\lambda)$  and  $f^j(\lambda)$ .

Then we calculated the transfer functions  $B_j(\lambda)$  ( $j = \text{red, green, blue}$ ) and the total and partial coherences for the smoothed Fourier series (Fig. 1). Smoothing is necessary because otherwise the individual frequency bins of the Fourier series are independent and the coherence would be equal to unity for all the bins.

The coherence squared in the g-mode range is roughly 0.8. This means that 80% of power in the TSI spectrum can be explained by the signals of the red, green and blue channels. We use this to reduce the solar

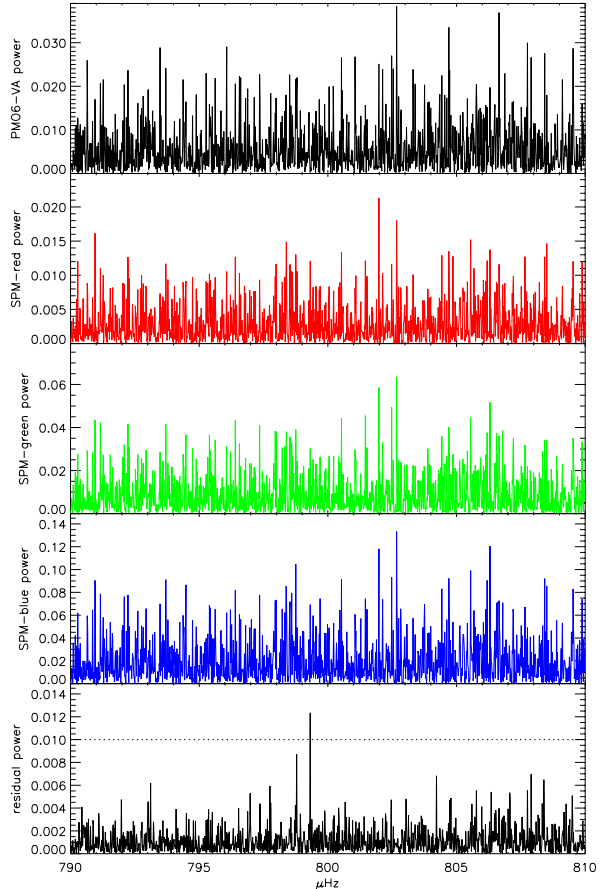


Figure 3. The top four panels show total and spectral solar irradiance power spectra in the range where we introduced an artificial mode of about 0.1 ppm. In the residual spectrum on the lowest panel the artificial mode appears as the highest peak, well above the dotted line, which indicates 90% significance level.

noise in the TSI spectrum by subtracting the filtered red, green and blue spectra (Eq. 10, Fig. 2). Almost all the power in the g-modes range ( $100 \sim 300 \mu\text{Hz}$ ) is due to solar meso-granulation. The contribution from the g modes to the total power is negligible and instrumental noise is low above  $100 \mu\text{Hz}$  (Anklin et al., 1998). The same is true for total coherence of total and spectral channels. In other words, the amount of power in the TSI spectrum, which is explained by the red, green and blue spectra, is mainly due to solar noise. This assumption holds only if the smoothing of the Fourier spectra runs over a sufficient large number of frequency bins. We applied a boxcar running mean of 101 bins  $\simeq 1.5 \mu\text{Hz}$  width, so the signal of an oscillation mode contributes with only 1% to the mean.

With the transfer functions  $B_j(\lambda)$  ( $j = \text{red, green, blue}$ ) according to Eq. 3 and  $f^t(\lambda)$  the original, not smoothed, TSI Fourier spectrum,  $F^t(\lambda)$  the noise reduced TSI Fourier spectrum can be calculated according to

$$F^t(\lambda) = f^t(\lambda) - \sum_{j=r,g,b} B_j(\lambda) f^j(\lambda) \quad (10)$$

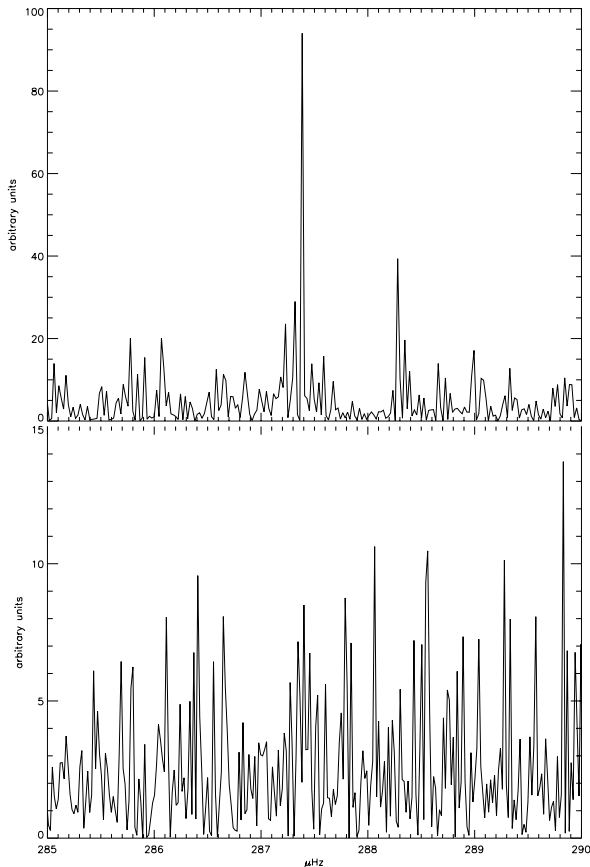


Figure 4. The two spikes on the upper panel are separated by roughly  $0.8 \mu\text{Hz}$ , which would be a reasonable value for rotational splitting of a  $p$  mode. Their central frequency lies about  $3.5 \mu\text{Hz}$  away from the predicted frequency of the  $p$  mode  $n = 1, l = 1$ . The same analysis performed on a 10% longer time series does not show these peaks anymore (lower panel, same units as upper panel). This leads to the conclusion that the two spikes in the upper panel are just due to differences in the instrumental noise between PMO6-VA and SPM. Inversions calculated by A. Kosovichev support this conclusion because the observed ‘ $p1$ ’ frequency would imply very large changes in the standard solar model (Fig. 5).

where  $f^j(\lambda)$  are the original, not smoothed, Fourier spectra of the red, green and blue channel of the SPM, respectively.

The fact, that the multivariate regression is more sensitive to uncorrelated meso-granulation than to coherent oscillation modes, can be used to discover modes that are hidden in the noise. As a test we introduced an artificial mode with constant frequency and an amplitude of about 0.1 ppm to the time series of total and spectral solar irradiance. The amplitude ratios between the different channels are chosen similar to the amplitude ratios of the 5-minutes oscillations. In the residual spectrum (bottom panel of Fig. 3) the ‘mode’ appears as a peak which is clearly above the 90% significance level. Note the reduction of noise by a factor of 5 according to  $\rho^2 = 0.8$ . But there are still rather high noise spikes remaining in the residual power which cannot be associated to solar oscillations. This indicates that the interpretation of remaining spikes has to be done with care.

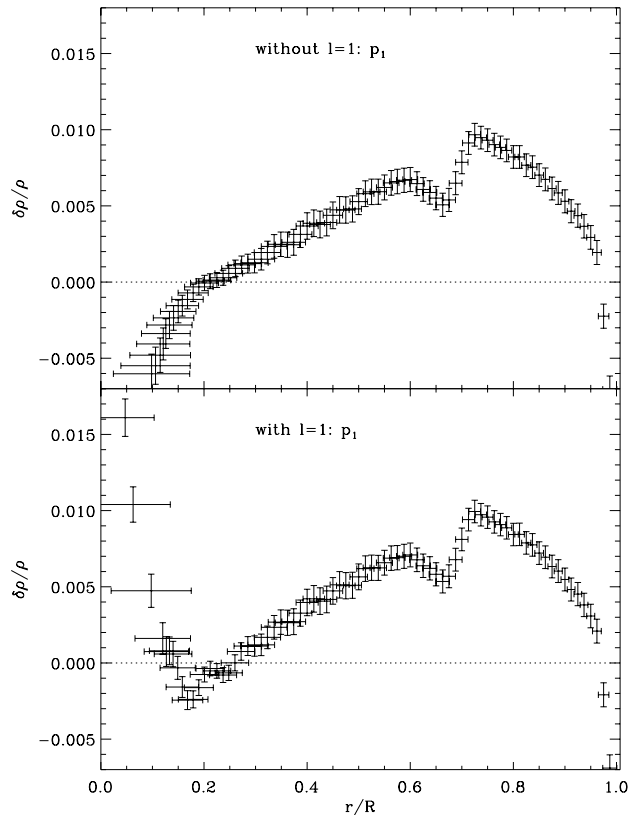


Figure 5. This plot shows the effect the ‘ $p1$ ’-frequency derived from Fig. 4 (upper panel) would imply to standard solar models. (provided by A. Kosovichev, 1998).

The reduction of noise is based on both the absolute value and phase relations between the dependent and independent spectra. Therefore peaks in the residual power can appear just because of amplitude or phase shifts between single Fourier coefficients of either the dependent or the independent spectra. Because the phase of a single Fourier coefficient is not very stable (i.e. it may vary strongly due to small changes in the time series), it may happen that peaks appear in the residual power just by chance. This was the case when we found a high spike close to the expected frequency of the  $p$  mode  $n = 1, l = 1$ . Only a very short period of additional data made the peak vanishing again (Fig. 4, 5). One therefore has to be very careful in interpreting the spikes, that appear in the power spectra because of constructive interference with noise.

### 3. SUMMARY

We have seen that multivariate spectral regression analysis is a strong tool to remove power from a spectrum. The method makes use of the coherent part in different components of a multivariate process. In our case we look at the variability of solar irradiance as a multivariate process which is sampled in total and spectral irradiance. Because mostly meso-granulation counts for the power, and hence the coherence, in the  $g$ -modes range, we can use multivariate regression to find spikes that do not come from the noise and may be hidden in the original

spectrum (Fig. 3). But we may as well be fooled by spikes that appear in the residual power because of the large phase shifts in the fourier spectrum produced by small instrumental effects in the time series. For the VIRGO data danger low as the instrumental noise in this range is very low. As we can see in Fig. 1 and 2, the total coherence between total and spectral irradiance is high and the noise level of the residual power is lower by a factor of about 5 with respect to the original spectrum. Some spikes are visible in the residual power which were hidden in the original spectrum. Unfortunately, they are due to incoherent instrumental noise in the total and spectral channels and not to g modes.

#### ACKNOWLEDGEMENTS

The authors gratefully acknowledge the past and ongoing effort of the VIRGO team to produce and interpret the data. SOHO is a mission of international cooperation between ESA and NASA. The work at PMOD/WRC is funded by the Swiss National Foundation.

#### REFERENCES

- Anklin, M., Fröhlich, C., Finsterle, W., and Wehrli, C.: 1998, in S. Korzenik and A. Wilson (eds.), *Structure and Dynamics of the Interior of the Sun and Sun-Like Stars*, p. this volume, ESA SP-418, ESA Publications Division, Noordwijk, The Netherlands
- Fröhlich, C., Andersen, B., Appourchaux, T., Berthomieu, G., Crommelynck, D. A., Domingo, V., Fichot, A., Finsterle, W., Gómez, M. F., Gough, D. O., Jiménez, A., Leifsen, T., Lombaerts, M., Pap, J. M., Provost, J., Roca Cortés, T., Romero, J., Roth, H., Sekii, T., Telljohann, U., Toutain, T., and Wehrli, C.: 1997, *Sol.Phys.* **170**, 1
- Koopmans, L. H.: 1974, *The Spectral Analysis of Time Series*, Academic Press, Inc., 111 Fifth Avenue, New York, NY 10003
- Kosovichev, A.: 1998, *Inversions of VIRGO and MDI Data*, <http://quake.Stanford.EDU:80/sasha/VIRGO/>